

RESEARCH ARTICLE

Complete Genome Sequence and Comparative Genomic Analysis of *Mycobacterium massiliense* JCM 15300 in the *Mycobacterium abscessus* Group Reveal a Conserved Genomic Island MmGI-1 Related to Putative Lipid Metabolism



CrossMark
click for updates

OPEN ACCESS

Citation: Sekizuka T, Kai M, Nakanaga K, Nakata N, Kazumi Y, et al. (2014) Complete Genome Sequence and Comparative Genomic Analysis of *Mycobacterium massiliense* JCM 15300 in the *Mycobacterium abscessus* Group Reveal a Conserved Genomic Island MmGI-1 Related to Putative Lipid Metabolism. PLoS ONE 9(12): e114848. doi:10.1371/journal.pone.0114848

Editor: Jean Louis Herrmann, Hopital Raymond Poincare - Universite Versailles St. Quentin, France

Received: February 27, 2014

Accepted: November 14, 2014

Published: December 11, 2014

Copyright: © 2014 Sekizuka et al. This is an open-access article distributed under the terms of the [Creative Commons Attribution License](http://creativecommons.org/licenses/by/4.0/), which permits unrestricted use, distribution, and reproduction in any medium, provided the original author and source are credited.

Funding: This work was supported in part by a Grant-in-Aid (25461178) for Scientific Research (C) from the Japan Society for the Promotion of Science (<http://www.jsps.go.jp/english/index.html>), by a grant from the Ohyama Health Foundation (<http://www.disclo-koeki.org/10a/01044/index.html>) and by a Grant-in-Aid (H25-Shinko-Ippan-015) from the Ministry of Health, Labour, and Welfare, Japan (<http://www.jsps.go.jp/english/e-grants/grants.html>). The funders had no role in study design, data collection and analysis, decision to publish, or preparation of the manuscript.

Competing Interests: Yoshihiko Hoshino is a PLOS ONE Editorial Board member. This does not alter the authors' adherence to all PLOS ONE policies on sharing data and materials, as detailed online in the guide for authors.

Tsuyoshi Sekizuka^{1*§}, **Masanori Kai**^{2§}, **Kazue Nakanaga**², **Noboru Nakata**², **Yuko Kazumi**³, **Shinji Maeda**³, **Masahiko Makino**², **Yoshihiko Hoshino**^{2*}, **Makoto Kuroda**¹

1. Pathogen Genomics Center, National Institute of Infectious Diseases, Tokyo, Japan, 2. Leprosy Research Center, National Institute of Infectious Diseases, Tokyo, Japan, 3. Research Institute of Tuberculosis, Japan Anti-Tuberculosis Association, Tokyo, Japan

*sekizuka@niid.go.jp (TS); yhoshino@niid.go.jp (YH)

§ These authors contributed equally to this work.

Abstract

Mycobacterium abscessus group subsp., such as *M. massiliense*, *M. abscessus sensu stricto* and *M. bolletii*, are an environmental organism found in soil, water and other ecological niches, and have been isolated from respiratory tract infection, skin and soft tissue infection, postoperative infection of cosmetic surgery. To determine the unique genetic feature of *M. massiliense*, we sequenced the complete genome of *M. massiliense* type strain JCM 15300 (corresponding to CCUG 48898). Comparative genomic analysis was performed among *Mycobacterium* spp. and among *M. abscessus* group subsp., showing that additional β -oxidation-related genes and, notably, the mammalian cell entry (*mce*) operon were located on a genomic island, *M. massiliense* Genomic Island 1 (MmGI-1), in *M. massiliense*. In addition, putative anaerobic respiration system-related genes and additional mycolic acid cyclopropane synthetase-related genes were found uniquely in *M. massiliense*. Japanese isolates of *M. massiliense* also frequently possess the MmGI-1 (14/44, approximately 32%) and three unique conserved regions (26/44; approximately 60%, 34/44; approximately 77% and 40/44; approximately 91%), as well as isolates of other countries (Malaysia, France, United Kingdom and United

States). The well-conserved genomic island MmGI-1 may play an important role in high growth potential with additional lipid metabolism, extra factors for survival in the environment or synthesis of complex membrane-associated lipids. ORFs on MmGI-1 showed similarities to ORFs of phylogenetically distant *M. avium* complex (MAC), suggesting that horizontal gene transfer or genetic recombination events might have occurred within MmGI-1 among *M. massiliense* and MAC.

Introduction

Nontuberculous mycobacteria (NTM) are classified into slowly growing mycobacterium (SGM) and rapidly growing mycobacterium (RGM) species; some of these bacteria cause pulmonary diseases [1]. Among RGM, the *Mycobacterium abscessus* group has been shown to be an emerging respiratory pathogen in cystic fibrosis, non-cystic-fibrosis bronchiectasis and chronic obstructive pulmonary disease [2, 3, 4, 5, 6], and is also an environmental organism found in soil, water and other ecological niches [7, 8]. The *M. abscessus* group consists of three subspecies, *M. abscessus* subsp. *abscessus* (*M. abscessus sensu stricto*), *M. abscessus* subsp. *massiliense* (*M. massiliense*) and *M. abscessus* subsp. *bolletii* (*M. bolletii*) [9, 10]. The three subspecies can generally be distinguished by phylogenetic analysis of the housekeeping gene, *rpoB*, and the macrolide resistance-related gene, erythromycin ribosome methyltransferase (*erm*) (41). Bryant *et al.* and Nakanaga *et al.* have recently reported more detailed classification methods, including, respectively, a whole-genome single nucleotide polymorphism (SNP) approach and a multiplex PCR method using insertion/deletion regions identified by whole-genome sequencing alignment analysis [4, 11]. Several subcutaneous infections following surgery, other medical treatments or traumatic injury have recently been found to be caused by *M. massiliense* [12, 13, 14, 15]. It was also recently reported that *M. massiliense* caused cutaneous infections that could not be attributed to a prior invasive procedure [16]. Phylogenetic analyses of the *M. abscessus* group have been performed, putative virulence factors of *M. abscessus sensu stricto* have been identified and studied, and the comparative whole-genome analysis of *M. abscessus* group isolated from patients of wide geographical origin have been performed [4, 17, 18, 19]; however, a detailed comparative analysis of *M. abscessus* group subspp. to determine *M. massiliense* unique genetic feature is lacking. Thus, in the current study, we sequenced the complete *M. massiliense* JCM 15300 (CCUG 48898) genome and compared it with that of *M. abscessus* group subspecies.

Results and Discussion

Genomic sequence of *M. massiliense* JCM 15300

The complete chromosomal sequence of *M. massiliense* JCM 15300 was obtained by *de novo* assembly of short reads followed by gap-closing using directed PCR. The genome consisted of 4,978,382 base pairs (bps) with a GC content of 64.1% and 4,950 predicted coding sequences (CDSs), 46 tRNA genes, one rRNA operon and two prophages (Fig. 1A). The chromosomal sequence corresponded to the predicted restriction fragment profiles obtained by PFGE analysis (data not shown). A draft genomic sequence of CCUG 48898 corresponding to JCM 15300 has been previously deposited in GenBank (NZ_AHAR01000000) by another research group. Thus, we performed a comparative pair-wise sequence alignment, revealing highly conserved synteny to the complete genomic sequence of JCM 15300 (S1 Figure and S1 Table). There were 188 mutations within 33 CDSs and 7 non-coding sites, suggesting that the differences between type strains may be due to frequent passaging and cultivation in various laboratories and bioresource centers. JCM15300 strain is smooth colony morphotype, and then there are no nonsense or frameshift mutations and in *mps1-mps2-gap* (MMASJCM_4183, MMASJCM_4184 and MMASJCM_4185) or *mmp14b* (MMASJCM_4202) (data not shown), these data is consistent with a previous report [20].

Comparative genomic analysis within the *Mycobacterium* genus

To characterize the genomic features of *M. massiliense* JCM 15300, a BLAST atlas analysis was performed; corresponding orthologs in complete and draft genomic sequences of other *Mycobacterium* spp. were compared with those of *M. massiliense* JCM 15300 as a reference (*M. bolletii* BD is a draft genomic sequence, but it is closely related to *M. massiliense*) (Fig. 1A). The BLAST atlas identified the conserved proteins in the core genome, which was represented by 973 CDSs (19.7%) shared among all 15 *Mycobacterium* spp. genomes. *M. massiliense* JCM 15300 was highly similar to *M. abscessus* ATCC 19977 and *M. bolletii* BD in the *M. abscessus* group (Fig. 1B). In contrast, *M. massiliense* JCM 15300 showed a low similarity (~73% of mean identity) to SGM and other RGM (Fig. 1B). The 16S rRNA phylogenetic analysis suggested complete identity of *M. massiliense* JCM 15300 to *M. abscessus* ATCC 19977 and *M. bolletii* BD (Fig. 1C). These results indicate that *M. massiliense* is difficult to distinguish among the three *M. abscessus* subspecies using 16S rRNA gene phylogeny and that the three subspecies belong to the *M. abscessus* group as suggested by many reports.

The above analysis demonstrated that there were several highly variable gene clusters and notable differences in GC content (64.1%) among the 14 *Mycobacterium* spp. One prophage, located in the region from 1,816 to 1,880 kbs, had a lower GC content (59.64%) and partially shared some conserved CDSs with *M. abscessus* ATCC 19977 (gray bar in the lower right of Fig. 1A). The average GC content of all 14 *Mycobacterium* spp. and 620 mycobacteriophages [21] was approximately 66% and 64%, respectively, suggesting that the low-GC content

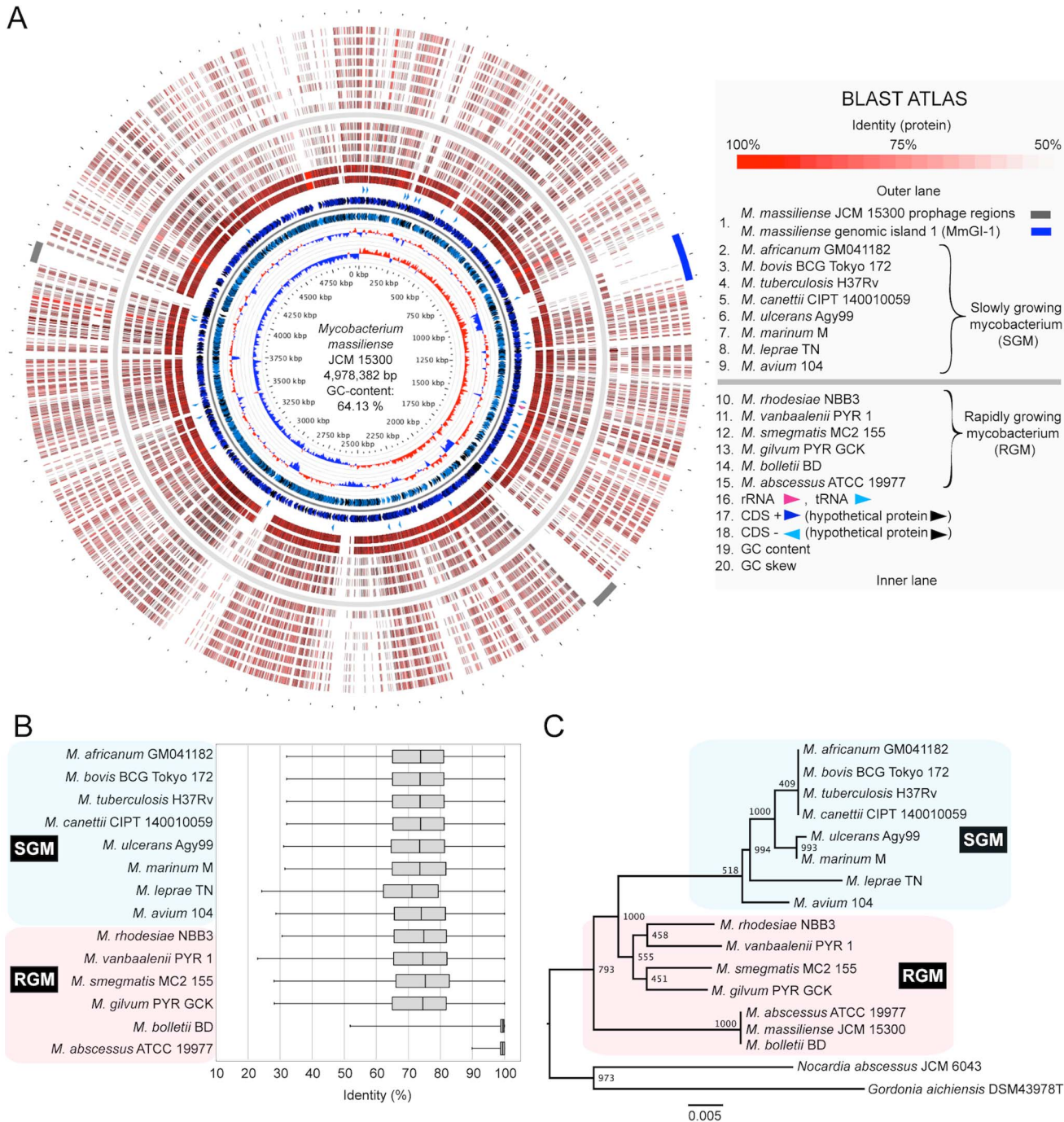


Fig 1. Circular representation of the *M. massiliense* JCM 15300 genome and comparative analysis among the complete genomes of *Mycobacterium* species. A. BLAST atlas of *M. massiliense* JCM 15300. The coding region of strain JCM 15300 was aligned against those of 14 other *Mycobacterium* genomes using BLASTP. The results are displayed as colored circles with increasing color intensity signifying increased similarity. It was estimated that the number of conserved proteins was 1,516 among all 14 *Mycobacterium* genomes. B. Box plot of identity percentage of conserved proteins between *M. massiliense* JCM 15300 and 14 other *Mycobacterium* spp. The top of each box in the box plot indicates the 75th percentile, the bottom of each box indicates the 25th percentile and the center bar represents the median. C. Neighbor-joining phylogenetic tree based on 16S rRNA gene sequencing of *Mycobacterium* with 1,000-fold bootstrapping. Scale bar indicates number of substitutions per site. The number at each branch node represents the bootstrapping value. *Nocardia abscessus* JCM 6043 (GenBank: AF430018) and *Gordonia aichiensis* DSM43978T (X80633) were used as outgroups.

doi:10.1371/journal.pone.0114848.g001

prophage was recently acquired. In contrast, another prophage, located in the region from 3,964,186 to 4,013,302 bps, had an average GC content (64%), indicating that it could be specific to *M. massiliense* JCM 15300 (gray bar in the upper left of [Fig. 1A](#)).

Intriguingly, a notable genomic island from 946,561 to 1,057,603 bps, designated *M. massiliense* genomic island 1 (MmGI-1; indicated by the blue bar in the upper right of [Fig. 1A](#)), appeared to be conserved among *M. massiliense* JCM 15300, *M. bolletii* BD and *M. avium* 104. The genomic island contained gene clusters associated with lipid metabolism and lipid-related transporters ([Fig. 2](#) and [Table 1](#)). β -oxidation-related genes were also identified, such as long-chain fatty acid-CoA ligase (MMASJCM_1018, MMASJCM_1019, MMASJCM_1028), acyl-CoA dehydrogenase (MMASJCM_1023, MMASJCM_1030, MMASJCM_1035, MMASJCM_1038), enoyl-CoA hydratase (MMASJCM_1008, MMASJCM_1009, MMASJCM_1010, MMASJCM_1022), 3-hydroxyacyl-CoA dehydrogenase (MMASJCM_1006, MMASJCM_1034), acyl-CoA thiolase (MMASJCM_1016, MMASJCM_1036) and acetyl-CoA acetyltransferase (MMASJCM_1014) ([Table 1](#)).

An ortholog of the mammalian cell entry (*mce*) operon (MMASJCM_0985 to _0992) was found in the genomic island ([Fig. 2](#) and [Table 1](#)). The *mce* operon of *Actinomycetales* species has been suggested to encode a subfamily of ATP-binding cassette (ABC) transporters that have a possible role in remodeling the cell envelope [[22](#)] and entry of the pathogen into non-phagocytic cells [[23](#)]. Although the function of the Mce protein family has not been clearly established, its members are believed to be membrane lipid transporters. For example, it has been demonstrated that the *mce4* operon is required for cholesterol utilization and uptake by *M. tuberculosis* [[24](#)] and *M. smegmatis* [[25](#)]. *M. massiliense* JCM 15300 contained 8 loci from the *mce* operon, and one *mce* operon on the MmGI-1 genomic island demonstrated approximately 99% similarity to that of *M. bolletii* BD and approximately 80% similarity to that of *M. avium* 104.

To characterize a provenance of MmGI-1 regions, the regions were subjected to BLASTN/BLASTP search against NCBI nt/nr databases excluding *M. abscessus* group sequences. Although the nucleotide search with BLASTN did not show notable homology to MmGI-1 region, the protein search with BLASTP showed that 105 ORFs on MmGI-1 showed significant similarity to ORFs of *Actinomycetales* with 32 to 95% identity. Of 105 ORFs, forty-two ORFs showed similarities to ORFs of phylogenetically distant *M. avium* complex (MAC) ([Fig. 3](#)), suggesting that the MmGI-1 region might have been acquired through horizontal gene transfer or genetic recombination events with MAC.

Using 55 draft genomic sequences from the *M. abscessus* group [[17](#)] and one complete genomic sequence from *M. massiliense* JCM 15300, variation among the genomic islands was investigated. The phylogeny of *M. abscessus* group strains was further characterized by identifying 203,267 SNPs in the commonly shared genomic sequence ([Fig. 2](#)). The SNP phylogenetic analysis identified three clusters (i.e., massiliense, bolletii and abscessus clusters) from the *M. abscessus* group, consistent with a previous report [[17](#)]. Phylogenetic and heatmap analyses

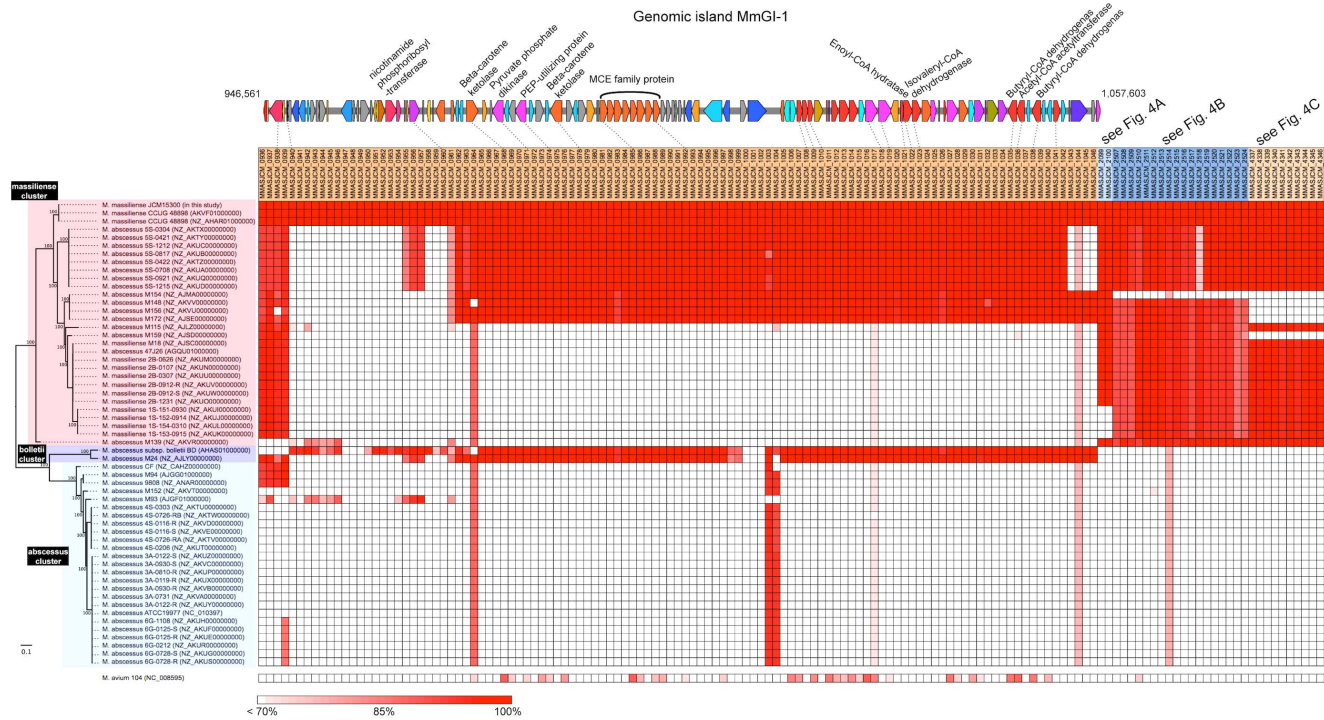


Fig. 2. Schematic representation of genomic island MmGI-1 and heatmap of MmGI-1, anaerobic respiration genes and mycolic acid synthase-related gene loci among 56 *M. abscessus* group strains. Phylogenetic tree based on 203,267 core genome SNPs in the whole-genome-sequenced *M. abscessus* group by the maximum-likelihood method with 1,000-fold bootstrapping. The scale indicates that a branch with a length of 0.1 is 10 times as long as one that would show a 1% difference between the nucleotide sequences at the beginning and end of the branch. The number at each branch node represents the bootstrapping value. The ORFs of *M. massiliense* strain JCM 15300 were aligned against the genomic sequences of 56 other *M. abscessus* group strains and *M. avium* 104 using TBLASTN (E-value cutoff, 1.00E-10; identity cutoff, 70%). A heatmap was constructed from amino acid identity.

doi:10.1371/journal.pone.0114848.g002

suggested that MmGI-1 was partially shared among *M. massiliense*-related strains (Fig. 2). Notably, the β -oxidation-related loci (MMASJCM_0982 to _1042) were also well conserved in *M. bolletii* BD and M24. These additional lipid-related metabolic genes may be important for high growth potential with additional lipid metabolism such as putative β -oxidation pathway, extra factors for survival in the environment (as suggested by the presence of MCE family protein) or synthesis of complex membrane-associated lipids (as suggested by the presence of a long-chain-fatty-acid-CoA ligase).

Comparative genomic analysis within the *M. abscessus* group
 To characterize the genomes of the previously described three clusters, we performed further comparative and BLAST atlas analyses based on the nucleotide sequences of two complete genomes and the predicted amino acid sequences of CDSs, respectively (S2 Figure and S2 and S3 Table), and then also performed pan-genomic analysis with 30 *M. massiliense*, 2 *M. bolletii* and 25 *M. abscessus* genome sequences because of a validation (S3 Figure). The pan-genomic analysis data is consistent with a previous report [19]. The comparative analysis yielded

Table 1. Genes on the genomic island MmGI-1 *M. massiliense* JCM 15300.

Gene_ID	Location at JCM 15300	Strand	Length	Product	COG classifications*	KEGG orthology	Accession number	Organisms	E-value	Identities
MMASJCM_0936	946561..947025	-	154	guanosine-3',5'-bis(Diphosphate) 3'-pyrophosphohydrolase	TK		WP_023955244.1	<i>Williamsia</i> sp. D3	7E-39	53.85%
MMASJCM_0937	947015..947167	-	50	hypothetical protein			WP_013871760.1	<i>Frankia</i> symbiont of <i>Datisca glomerata</i>	4E-06	47.73%
MMASJCM_0938	947284..949143	-	619	hypothetical protein	H		EUA75642.1	<i>M. chelonae</i> 1518	6E-161	69.98%
MMASJCM_0939	949143..949457	-	104	hypothetical protein	S		EUA75643.1	<i>M. chelonae</i> 1518	4E-22	54.74%
MMASJCM_0940	949859..950386	-	175	hypothetical protein			WP_015388818.1	<i>M. yongonense</i>	1E-72	66.27%
MMASJCM_0941	950404..951273	-	289	hypothetical protein	O		WP_023363492.1	<i>M. kansasii</i>	8E-67	49.62%
MMASJCM_0942	951280..952167	-	295	hypothetical protein	L		WP_023363490.1	<i>M. kansasii</i>	3E-118	62.93%
MMASJCM_0943	952344..952706	+	120	hypothetical protein	K		WP_015388820.1	<i>M. yongonense</i>	6E-37	68.42%
MMASJCM_0944	952851..953441	+	196	hypothetical protein			WP_015388821.1	<i>M. yongonense</i>	3E-54	61.96%
MMASJCM_0945	953484..954032	+	182	hypothetical protein			WP_015388822.1	<i>M. yongonense</i>	1E-69	58.56%
MMASJCM_0946	954019..955020	+	333	hypothetical protein			WP_015388823.1	<i>M. yongonense</i>	2E-154	72.50%
MMASJCM_0947	955027..955311	-	94	hypothetical protein	S		EWT07839.1	<i>Intrasporangium chromatireducens</i> Q5-1	2E-34	64.89%
MMASJCM_0948	956934..958430	-	498	site-specific DNA-methyltransferase	L		WP_020097565.1	<i>Microbacterium</i> sp. 11MF	7E-177	63.77%
MMASJCM_0949	958473..958796	+	107	hypothetical protein			WP_011768395.1	<i>Mycobacterium</i> sp. KMS	3E-08	36.56%
MMASJCM_0950	958893..959312	-	139	hypothetical protein			WP_006339348.1	<i>Gordonia rhizosphaera</i>	1E-14	31.85%
MMASJCM_0951	959512..960780	+	422	hypothetical protein			WP_029121465.1	<i>Mycobacterium</i> sp. UNC410CL29C-vi84	1E-165	58.18%
MMASJCM_0952	960806..961159	+	117	hypothetical protein			WP_020099065.1	<i>Mycobacterium</i>	5E-36	58.49%
MMASJCM_0953	961156..961461	-	101	hypothetical protein	S		WP_024801663.1	<i>Nocardia</i> sp. BMG51109	2E-09	35.42%
MMASJCM_0954	961458..961751	-	97	hypothetical protein	S		WP_020099063.1	<i>Mycobacterium</i>	2E-19	48.45%
MMASJCM_0955	961838..962734	+	298	phosphoribosylpyrophosphate synthetase	FE		ETB46104.1	<i>M. avium</i> 10-5560	2E-48	51.56%
MMASJCM_0956	962749..964272	+	507	nicotinamide phosphoribosyltransferase	H	K03462	ETB46369.1	<i>M. avium</i> 10-5560	0	71.69%

Table 1. Cont.

Gene_ID	Location at JCM 15300	Strand	Length	Product	COG classifications*	KEGG orthology	BLASTP top hit sequence (E-value cutoff: 1E-1, database: nr without <i>M. abscessus</i> group data)			
							Accession number	Organisms	E-value	Identities
MMASJCM_0957	964269..964919	+	216	possible DNA hydrolase	F	K03574	ETB46388.1	<i>M. avium</i> 10-5560	2E-66	53.00%
MMASJCM_0958	965195..965308	+	37	hypothetical protein			No hits found			
MMASJCM_0959	965479..965808	+	109	hypothetical protein	R		No hits found			
MMASJCM_0960	965980..967356	+	458	hypothetical protein	C		WP_0244449466.1	<i>M. iranicum</i>	0	57.42%
MMASJCM_0961	967635..967844	-	69	hypothetical protein			WP_015388818.1	<i>M. yongonense</i>	9E-23	75.38%
MMASJCM_0962	968295..968783	-	162	hypothetical protein	S		WP_025089036.1	<i>Mycobacterium</i>	6E-47	50.00%
MMASJCM_0963	968949..969167	-	72	hypothetical protein			WP_015291571.1	<i>M. canettii</i>	5E-13	60.71%
MMASJCM_0964	969380..970636	-	418	putative cytochrome P450 IgrA	Q	K00517	EUA78264.1	<i>M. chelonae</i> 1518	0	88.04%
MMASJCM_0965	971395..971925	+	176	conserved hypothetical integral membrane protein YrbE1A	Q		WP_005143639.1	<i>M. rhodesiae</i>	1E-37	44.97%
MMASJCM_0966	971981..972526	-	181	transcriptional regulator, TetR family	K		WP_014384296.1	<i>M. intracellulare</i>	5E-53	50.00%
MMASJCM_0967	972591..973097	-	168	transcriptional regulator, TetR family	K		WP_014384297.1	<i>M. intracellulare</i>	2E-61	58.33%
MMASJCM_0968	973468..975162	+	564	beta-carotene ketolase	Q	K02292	CDO90343.1	<i>M. triplex</i>	0	91.41%
MMASJCM_0969	975672..976337	+	221	hypothetical protein	R		CDO30896.1	<i>M. vulneris</i>	5E-120	74.21%
MMASJCM_0970	976573..976902	+	109	hypothetical protein			WP_010228994.1	<i>Pseudonocardia</i> sp. P1	5E-27	52.88%
MMASJCM_0971	976927..978438	-	503	pyruvate, phosphate dikinase	G	K01006	WP_011726421.1	<i>M. avium</i>	0	72.06%
MMASJCM_0972	978435..979052	-	205	hypothetical protein	K		KDO99916.1	<i>M. avium</i> subsp. <i>hominissuis</i> 101	1E-95	67.80%
MMASJCM_0973	979096..980010	-	304	hypothetical protein			WP_011726419.1	<i>M. avium</i>	2E-177	79.28%
MMASJCM_0974	980007..981524	-	505	hypothetical protein	G	K01007	KBR61967.1	<i>M. tuberculosis</i> XTB13-223	0	73.76%
MMASJCM_0975	981770..982378	+	202	transcriptional regulator, TetR family	K		WP_011726417.1	<i>M. avium</i>	1E-85	66.67%
MMASJCM_0976	982618..983658	+	346	hypothetical protein			CDO30900.1	<i>M. vulneris</i>	0	87.32%
MMASJCM_0977	983932..984459	+	175	transcriptional regulator, TetR family	K		CDO90192.1	<i>M. triplex</i>	2E-61	60.00%
MMASJCM_0978	984571..986193	-	540	beta-carotene ketolase	Q		KDE98300.1	<i>M. aromaticivorans</i> JS19b1	0	82.45%
MMASJCM_0979	986685..987560	+	291	hypothetical protein			KDE98305.1	<i>M. aromaticivorans</i> JS19b1	2E-175	83.74%
MMASJCM_0980	987577..988209	-	210	transcriptional regulator, TetR family	K		KDE98304.1	<i>M. aromaticivorans</i> JS19b1	1E-95	76.60%

Table 1. Cont.

Gene_ID	Location at JCM 15300	Strand	Length	Product	COG classifications*	KEGG orthology	BLASTP top hit sequence (E-value cutoff: 1E-1, database: nr without <i>M. abscessus</i> group data)			
							Accession number	Organisms	E-value	Identities
MMASJCM_0981	988316..989380	+	354	hypothetical protein			KDE98303.1	<i>M. aromaticivorans</i> JS19b1	0	77.68%
MMASJCM_0982	989396..990508	+	370	putative phosphotransferase	R		WP_005141265.1	<i>M. rhodesiae</i>	0	75.41%
MMASJCM_0983	990691..990807	+	38	hypothetical protein			No hits found			
MMASJCM_0984	990970..991083	-	37	hypothetical protein			No hits found			
MMASJCM_0985	991197..992228	+	343	putative YrbE family protein	Q		KBR61969.1	<i>M. tuberculosis</i> XTB13-223	2E-148	88.21%
MMASJCM_0986	992228..993097	+	289	putative Mce family protein	Q		KBR61970.1	<i>M. tuberculosis</i> XTB13-223	8E-168	80.28%
MMASJCM_0987	993105..994199	+	364	putative Mce family protein	Q		CDO30921.1	<i>M. vulneris</i>	0	70.56%
MMASJCM_0988	994196..995203	+	335	putative Mce family protein	Q		WP_011726414.1	<i>M. avium</i>	0	75.52%
MMASJCM_0989	995221..996162	+	313	putative Mce family protein	Q		KBR61973.1	<i>M. tuberculosis</i> XTB13-223	1E-176	77.96%
MMASJCM_0990	996132..997280	+	382	putative Mce family protein	Q		KDO39908.1	<i>M. avium</i> subsp. <i>hominissuis</i> 101	0	67.28%
MMASJCM_0991	997277..998266	+	329	putative Mce family protein	Q		WP_024637000.1	<i>M. avium</i>	2E-162	69.39%
MMASJCM_0992	998263..999219	+	318	putative Mce family protein	Q		CDO30926.1	<i>M. vulneris</i>	3E-157	69.50%
MMASJCM_0993	999262..999906	+	214	hypothetical protein			WP_007170571.1	<i>M. parascrofulaceum</i>	1E-82	61.27%
MMASJCM_0994	999982..1000584	+	200	hypothetical protein			KDE98251.1	<i>M. aromaticivorans</i> JS19b1	5E-88	65.83%
MMASJCM_0995	1000670..1001113	+	147	hypothetical protein			CDO30929.1	<i>M. vulneris</i>	7E-48	63.20%
MMASJCM_0996	1001158..1001496	+	112	hypothetical protein			WP_007170568.1	<i>M. parascrofulaceum</i>	4E-44	62.39%
MMASJCM_0997	1001544..1002104	+	186	hypothetical protein			CDO30931.1	<i>M. vulneris</i>	5E-91	75.71%
MMASJCM_0998	1002279..1002410	+	43	hypothetical protein			No hits found			
MMASJCM_0999	1002407..1003372	-	321	hypothetical protein	O		WP_014711294.1	<i>Mycobacterium</i> sp. MOTT36Y	0	80.94%
MMASJCM_1000	1003379..1004497	-	372	putative phosphotransferase	R		CDO90200.1	<i>M. triplex</i>	0	68.01%
MMASJCM_1001	1004938..1007496	-	852	hypothetical protein	K		WP_030203671.1	<i>Pilimella anulata</i>	0	72.98%

Table 1. Cont.

Gene_ID	Location at JCM 15300	Strand	Length	Product	COG classifications*	KEGG orthology	BLASTP top hit sequence (E-value cutoff: 1E-1, database: nr without <i>M. abscessus</i> group data)			Identities
							Accession number	Organisms	E-value	
MMASJCM_1002	1007489..1008457	-	322	cell division protein FtsH	O		WP_022566726.1	<i>Nocardia asteroides</i>	0	88.51%
MMASJCM_1003	1009865..1010737	+	290	hypothetical protein			EUA78068.1	<i>M. chelonae</i> 1518	4E-180	95.32%
MMASJCM_1004	1010796..1013315	+	839	hypothetical protein	D		WP_005113273.1	<i>M. chelonae</i>	0	94.89%
MMASJCM_1005	1015076..1015558	-	160	hypothetical protein	Q		WP_013873946.1	Frankia symbiont of <i>Datisca glomerata</i>	3E-23	45.45%
MMASJCM_1006	1015591..1016388	-	265	2-hydroxycyclohexanecarboxyl-CoA dehydrogenase	IQR		WP_011726451.1	<i>M. avium</i>	1E-162	83.77%
MMASJCM_1007	1016500..1017249	+	249	3-oxoacyl-[acyl-carrier protein] reductase	IQR		WP_023985895.1	<i>M. neoaurum</i>	2E-135	80.82%
MMASJCM_1008	1017246..1018016	+	256	enoyl-CoA hydratase	I		WP_011726449.1	<i>M. avium</i>	8E-104	66.54%
MMASJCM_1009	1018013..1018810	+	265	enoyl-CoA hydratase	I		WP_011726448.1	<i>M. avium</i>	4E-145	82.95%
MMASJCM_1010	1018810..1019595	+	261	enoyl-CoA hydratase	I		WP_029114372.1	<i>Mycobacterium</i> sp. URHB0044	7E-120	70.93%
MMASJCM_1011	1019592..1020860	+	422	putative dioxygenase hydroxylase component	PR		WP_030136631.1	<i>M. neoaurum</i>	0	86.46%
MMASJCM_1012	1021187..1021393	+	68	beta subunit of hydroxylase component of benzoate 1,2-dioxygenase	Q		WP_011726445.1	<i>M. avium</i>	3E-26	77.05%
MMASJCM_1013	1021459..1021659	+	66	hypothetical protein	T		WP_030136633.1	<i>M. neoaurum</i>	3E-29	81.54%
MMASJCM_1014	1021938..1022864	+	308	acetyl-CoA acetyltransferase	I		WP_014384231.1	<i>M. intracellulare</i>	0	84.36%
MMASJCM_1015	1022861..1024216	+	451	hydroxymethylglutaryl-CoA synthase	I		WP_011726442.1	<i>M. avium</i>	0	73.38%
MMASJCM_1016	1024206..1025411	+	401	putative thiolase	I		WP_011726441.1	<i>M. avium</i>	0	88.35%
MMASJCM_1017	1025490..1026350	+	286	probable short-chain type dehydrogenase reductase	IQR		WP_011726440.1	<i>M. avium</i>	4E-172	84.27%
MMASJCM_1018	1026409..1028046	+	545	long-chain-fatty-acid-CoA ligase	IQ		WP_011726439.1	<i>M. avium</i>	0	66.42%
MMASJCM_1019	1028043..1029800	+	585	long-chain-fatty-acid-CoA ligase	IQ		WP_011726438.1	<i>M. avium</i>	0	68.67%

Table 1. Cont.

Gene_ID	Location at JCM 15300	Strand	Length	Product	COG classifications*	KEGG orthology	BLASTP top hit sequence (E-value cutoff: 1E-1, database: nr without <i>M. abscessus</i> group data)			
							Accession number	Organisms	E-value	Identities
MMASJCM_1020	1029761..1030786	-	341	hypothetical protein	R		WP_023985889.1	<i>M. neoaurum</i>	7E-128	57.19%
MMASJCM_1021	1030966..1031418	+	150	acyl dehydratase	I		WP_003923910.1	<i>M. thermoresis-tibile</i>	2E-76	75.00%
MMASJCM_1022	1031408..1032619	+	403	enoyl-CoA hydratase	I	K15866	WP_007170622.1	<i>M. parascrofulaceum</i>	2E-174	67.74%
MMASJCM_1023	1032620..1033783	+	387	isovaleryl-CoA dehydrogenase	I		WP_007170621.1	<i>M. parascrofulaceum</i>	0	81.61%
MMASJCM_1024	1033815..1035116	+	433	phytoene dehydrogenase family protein	Q		WP_007170620.1	<i>M. parascrofulaceum</i>	0	81.73%
MMASJCM_1025	1035104..1035961	+	285	citrate lyase beta chain	G	K01644	WP_007170619.1	<i>M. parascrofulaceum</i>	9E-111	66.92%
MMASJCM_1026	1036061..1036291	-	76	hypothetical protein			No hits found			
MMASJCM_1027	1036800..1037204	+	134	hypothetical protein	I		CDO90349.1	<i>M. triplex</i>	4E-79	88.06%
MMASJCM_1028	1037208..1038746	+	512	long-chain-fatty-acid—CoA ligase	IQ	K00666	WP_030136653.1	<i>M. neoaurum</i>	0	76.32%
MMASJCM_1029	1038743..1040002	+	419	putative cytochrome P450 hydroxylase	Q	K00517	CDO30946.1	<i>M. vulneris</i>	0	90.31%
MMASJCM_1030	1040014..1040805	+	263	3-alpha-hydroxysteroid dehydrogenase	IQR		WP_019509868.1	<i>M. neoaurum</i>	9E-156	82.89%
MMASJCM_1031	1040815..1042215	+	466	aldehyde dehydrogenase	C	K00128	WP_003923898.1	<i>M. thermoresis-tibile</i>	0	75.28%
MMASJCM_1032	1042215..1042406	+	63	hypothetical protein	C		WP_005141491.1	<i>M. rhodesiae</i>	3E-19	66.13%
MMASJCM_1033	1042569..1044056	+	495	ferredoxin—NADP(+) reductase	ER	K00528	KBR61952.1	<i>M. tuberculosis</i> XTB13-223	0	64.02%
MMASJCM_1034	1044016..1045248	+	410	4-hydroxybutyrate coenzyme A transferase	C		WP_011726433.1	<i>M. avium</i>	0	69.07%
MMASJCM_1035	1045317..1046471	-	384	butyryl-CoA dehydrogenase	I		WP_019509874.1	<i>M. neoaurum</i>	0	84.03%
MMASJCM_1036	1046475..1047626	-	383	acetyl-CoA acetyltransferase	I	K07823	WP_011726431.1	<i>M. avium</i>	0	87.21%
MMASJCM_1037	1047688..1048263	-	191	transcriptional regulator, TetR family	K		WP_030136662.1	<i>M. neoaurum</i>	6E-93	71.96%
MMASJCM_1038	1048446..1049600	-	384	butyryl-CoA dehydrogenase	I	K00248	WP_014941082.1	<i>M. indicus pranii</i>	0	84.38%
MMASJCM_1039	1049725..1050264	-	179	transcriptional regulator, TetR family	K		WP_019509888.1	<i>M. neoaurum</i>	3E-67	60.12%

Table 1. Cont.

Gene_ID	Location at JCM 15300	Strand	Length	Product	COG classifications*	KEGG orthology	BLASTP top hit sequence (E-value cutoff: 1E-1, database: nr without <i>M. abscessus</i> group data)			
							Accession number	Organisms	E-value	Identities
MMASJCM_1040	1050416..1051048	-	210	transcriptional regulator, TetR family	K		WP_005146732.1	<i>M. rhodesiae</i>	6E-102	74.00%
MMASJCM_1041	1051285..1052259	+	324	hypothetical protein	I		WP_003938179.1	<i>Rhodococcus ruber</i>	5E-121	60.67%
MMASJCM_1042	1052411..1053019	+	202	transcriptional regulator, TetR family protein, putative	K		WP_014384219.1	<i>M. intracellulare</i>	5E-97	71.14%
MMASJCM_1043	1053327..1053584	+	85	hypothetical protein			WP_005111625.1	<i>M. chelonae</i>	2E-21	58.54%
MMASJCM_1044	1053701..1055929	+	742	carbonic anhydrase	P	K01673	WP_005057131.1	<i>M. chelonae</i>	0	76.16%
MMASJCM_1045	1056430..1056960	+	176	hypothetical protein			WP_028655880.1	<i>Nocardioides</i> sp. J54	2E-11	32.62%
MMASJCM_1046	1057007..1057603	+	198	hypothetical protein	G		WP_003960345.1	<i>Streptomyces clavuligerus</i>	2E-05	37.18%

*COG codes is as follows: C: Energy production and conversion, D: Cell cycle control, cell division, chromosome partitioning, E: Amino acid transport and metabolism, F: Nucleotide transport and metabolism, G: Carbohydrate transport and metabolism, H: Coenzyme transport and metabolism, I: Lipid transport and metabolism, J: Inorganic ion transport and metabolism, K: Transcription, L: Replication, recombination and repair, O: Posttranslational modification, protein turnover, chaperones, P: Inorganic ion transport and metabolism, Q: Secondary metabolites biosynthesis, transport and catabolism, R: General function prediction only, S: Function unknown, T: Signal transduction mechanisms.

doi:10.1371/journal.pone.0114848.t001

the following four results: i) as a massiliense cluster-specific feature, there were six unique regions (\dagger^{1-6} in [S2 Figure](#) and [Table 2](#)) that contained an average GC content of 64%; ii) as a JCM 15300-specific feature, there were 10 unique regions (\bullet in [S2 Figure](#) and [S2 Table](#)) that had relatively low GC content; iii) the MmGI-1 genomic island ([Fig. 3](#) and \P in [S2 Figure](#)) was shared with *M. bolletii* and showed partial similarity to *M. avium* 104; iv) there were two common deletions (\dagger^{7-8} in [S2 Figure](#) and [S3 Table](#)) in the massiliense cluster and one conserved region in the abscessus group (\S in [S2 Figure](#) and [S3 Table](#)).

In addition to the MmGI-1 genomic island described above, the massiliense cluster contained three notable conserved loci: i) a molybdopterin oxidoreductase ([Fig. 2](#), [Fig. 4A](#) and [Table 2](#)); ii) universal stress proteins, an alcohol dehydrogenase and a xylulose-5-phosphate phosphoketolase ([Fig. 2](#), [Fig. 4B](#) and [Table 2](#)); iii) a cyclopropane fatty acyl-phospholipid synthase and an S-adenosyl-L-methionine-dependent methyltransferase ([Fig. 2](#), [Fig. 4C](#) and [Table 2](#)). In contrast to MmGI-1, these three regions were well conserved within the massiliense cluster.

Choo *et al.* previously reported that a high proportion of accessory strain-specific genes indicating an open, non-conservative pan-genome structure, and clear evidence of rapid phage-mediated evolution [19]. In fact, specific genes in *M. massiliense* JCM15300 contained phage-related genes, i.e. putative prophage integrase ([S2 Table](#)). On the other hand, in adjacent gene loci of three conserved regions, i.e. MMASJCM-2099..2100, MMASJCM-2507..2524 and MMASJCM-4337..4346, there are no phage-related genes ([Fig. 4](#) and [Table 2](#)). These data suggest that these conserved regions might be core-genome regions in ancestral *M. abscessus* group, and then have been deleted from genomes of *M. abscessus* and *M. bolletii*.

Prevalence of MmGI-1 and massiliense cluster unique regions in Japanese *M. massiliense* and *M. abscessus* isolates

We examined the prevalence of MmGI-1 and three massiliense cluster unique regions in Japanese *M. massiliense* and *M. abscessus* isolates using conventional PCR methods ([S4 Table](#)), because of *in silico* analysis using only isolates of Malaysia, France, United Kingdom and United States. The ratio of MmGI-1 positive *M. massiliense* and *M. abscessus* was 31.8% (14/44) and 1.4% (1/70), respectively ([Fig. 5A](#) and [S5 Table](#)). Applying Fisher's exact test, the proportion of MmGI-1 positive *M. massiliense* is significantly higher than that of *M. abscessus* ($P=0.0001$). *M. massiliense* frequently possesses three massiliense cluster unique regions in not only Japanese but also other countries (Malaysia, France and United States) isolates ([Fig. 5A](#) and [S5 Table](#)), suggesting that MmGI-1 and the massiliense cluster unique regions are highly conserved in *M. massiliense* isolated from various countries.

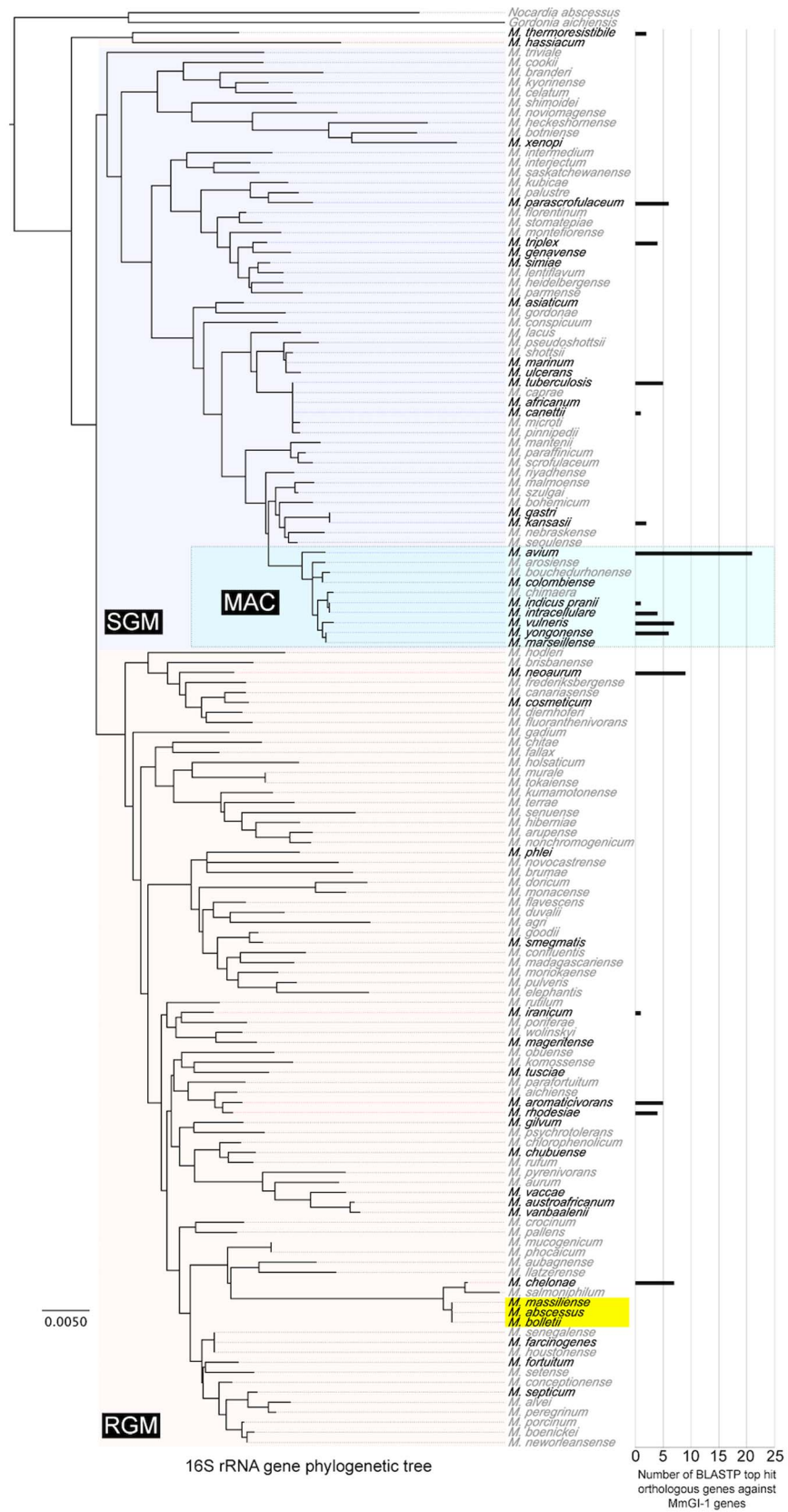


Fig. 3. Orthologous genes of MmGI-1 genes in *Mycobacterium* spp. without *M. abscessus* group. Phylogenetic tree based on the 16S rRNA was constructed by Neighbor-joining method with 1,000-fold bootstrapping. Scale bar indicates number of substitutions per site. Species of black characters indicate that complete or draft genome sequences have been deposited at DDBJ/EMBL/GenBank. *M. abscessus* group is labeled by a yellow box. The number of BLASTP top hit orthologous genes against MmGI-1 genes are shown with a right bar chart.

doi:10.1371/journal.pone.0114848.g003

Growth ability of MmGI-1 positive *M. massiliense*

The massiliense cluster contained a conserved molybdopterin oxidoreductase as described above, and an ortholog was also identified in the strictly anaerobic bacterium, *Desulfitobacterium hafniense*. It has been reported that molybdopterin oxidoreductase may provide the ability for anaerobic energy metabolism [26]. The xylulose-5-phosphate phosphoketolase may play a role in heterolactic fermentation in anaerobic heterolactic acid bacteria, including *Lactobacillus* and *Leuconostoc* organisms [27]. Moreover, the universal stress protein in *Pseudomonas aeruginosa* has been reported to have a crucial role in survival under anaerobic conditions [28]. These studies suggest that *M. massiliense* may grow or survive under anaerobic or hypoxic conditions. Indeed, the oxygen partial pressure in various tissues is approximately 20–50 mm Hg (3–7% oxygen) [29, 30, 31, 32]. To determine growth ability under hypoxic conditions, 27 smooth colony morphology isolates (12 *M. abscessus*, 8 MmGI-1 positive *M. massiliense* and 7 MmGI-1 negative *M. massiliense* isolates) were subjected to aerobic and microaerobic (approximately 6% O₂) conditions (Fig. 5B and 5C), because the aggregation of rough colony morphology isolates were hard to measure the degree of turbidity in the broth culture. In aerobic condition, MmGI-1 positive *M. massiliense* isolates show well growth than MmGI-1 negative isolates including *M. abscessus* (Fig. 5B). On the other hand, in microaerobic condition, the growth didn't show significant differences between *M. massiliense* and *M. abscessus* (Fig. 5C). MMASJCM-2099..2100 and MMASJCM-2057..2524 regions highly conserved in *M. massiliense* isolated from Japan, Malaysia, France, United Kingdom and United States, as well as MmGI-1. Although functions of these regions are still unclear, the importance of MmGI-1 might be supported by the existence on these conserved regions in *M. massiliense*, and MmGI-1 might relate to high growth potential with additional lipid metabolism such as putative β -oxidation pathway.

Phylogenetic analysis of mycolic acid synthase-related genes

The comparative genomic analysis indicated that *M. massiliense* including Japanese isolates possessed two extra CDSs that are possibly involved in the cyclopropanation of mycolic acid. A cyclopropane fatty acyl-phospholipid synthase (MMASJCM_4340) and an S-adenosyl-L-methionine-dependent methyltransferase (MMASJCM_4343) were detected only in the massiliense cluster (Fig. 4C). Both putative proteins encoded by these CDSs possessed the mycolic acid cyclopropane synthetase (CMAS) domain (pfam02353).

Table 2. The unique conserved gene loci in massiliense cluster among *M. abscessus* group.

Gene_ID	Location at JCM 15300	Strand	Length	Product	Note
MMASJCM_0834	825792..826802	-	336	transcriptional regulator	
MMASJCM_0835	826913..827713	+	266	short chain dehydrogenase	
MMASJCM_2099	2098058..2101435	-	1125	putative molybdopterin oxidoreductase	see Fig. 4A
MMASJCM_2100	2101513..2102112	+	199	putative transcriptional regulator	see Fig. 4A
MMASJCM_2410	2427416..2427601	-	61	hypothetical protein	
MMASJCM_2411	2427632..2428042	+	136	hypothetical protein	
MMASJCM_2412	2428054..2428788	+	244	hypothetical protein	
MMASJCM_2507	2509971..2510735	-	254	universal stress protein family	see Fig. 4B
MMASJCM_2508	2510875..2511216	-	113	universal stress protein family	see Fig. 4B
MMASJCM_2509	2511996..2512505	+	169	probable conserved transmembrane protein	see Fig. 4B
MMASJCM_2510	2512542..2513558	+	338	alcohol dehydrogenase	see Fig. 4B
MMASJCM_2511	2513572..2514579	-	335	hypothetical protein	see Fig. 4B
MMASJCM_2512	2514754..2515698	+	314	universal stress protein family	see Fig. 4B
MMASJCM_2513	2515695..2518106	+	803	xylulose-5-phosphate phosphoketolase	see Fig. 4B
MMASJCM_2514	2518103..2518852	+	249	two component transcriptional regulatory protein DevR	see Fig. 4B
MMASJCM_2515	2518819..2519823	+	334	sensor kinase	see Fig. 4B
MMASJCM_2516	2519946..2520536	+	196	histidine kinase response regulator	see Fig. 4B
MMASJCM_2517	2520544..2521497	+	317	sulfate transporter	see Fig. 4B
MMASJCM_2518	2521466..2522251	+	261	sulfate transporter	see Fig. 4B
MMASJCM_2519	2522241..2522855	-	204	hypothetical protein	see Fig. 4B
MMASJCM_2520	2522957..2523163	-	68	hypothetical protein	see Fig. 4B
MMASJCM_2521	2523183..2524058	-	291	universal stress protein family	see Fig. 4B
MMASJCM_2522	2524296..2525168	+	290	universal stress protein family	see Fig. 4B
MMASJCM_2523	2525188..2525475	+	95	hypothetical protein	see Fig. 4B
MMASJCM_2524	2525508..2525942	+	144	hypothetical protein	see Fig. 4B
MMASJCM_2869	2886124..2887602	+	492	carotenoid oxygenase	
MMASJCM_2870	2887612..2888793	+	393	two-component system	
MMASJCM_2871	2888790..2889410	+	206	two component transcriptional regulator	
MMASJCM_2872	2890468..2892372	-	634	hypothetical protein	
MMASJCM_2989	3016494..3018116	+	540	diaminopimelate decarboxylase	
MMASJCM_3589	3593912..3594541	-	209	transcriptional regulator	
MMASJCM_3590	3594814..3595809	+	331	2-amino-3-carboxymuconate-6-semialdehyde decarboxylase	
MMASJCM_4337	4335727..4337094	-	455	deoxyribodipyrimidine photolyase	see Fig. 4C
MMASJCM_4338	4337091..4338449	-	452	cell division inhibitor	see Fig. 4C
MMASJCM_4339	4338477..4339142	-	221	hypothetical protein	see Fig. 4C
MMASJCM_4340	4339165..4340058	-	297	cyclopropane-fatty-acyl-phospholipid synthase	see Fig. 4C
MMASJCM_4341	4340280..4341596	+	438	amine oxidase	see Fig. 4C
MMASJCM_4342	4341593..4342330	+	245	hypothetical protein	see Fig. 4C
MMASJCM_4343	4342327..4343601	+	424	S-adenosyl-L-methionine dependent methyltransferase	see Fig. 4C
MMASJCM_4344	4343598..4344383	+	261	hypothetical protein	see Fig. 4C
MMASJCM_4345	4344416..4344961	+	181	RNA polymerase sigma-70 factor	see Fig. 4C
MMASJCM_4346	4344943..4345665	+	240	hypothetical protein	see Fig. 4C

doi:10.1371/journal.pone.0114848.t002

Mycobacterium spp. possess 3 to 10 paralogs with a CMAS domain; for example, CmaA (cyclopropane mycolic acid synthase) and MmaA (methyl mycolic acid synthase) have been well characterized [33]. A phylogenetic analysis of CMAS domain-related proteins has indicated that one of the two extra proteins, MMASJCM_4340, is orthologous to MSMEG_1351 of *M. smegmatis* and MycrhN_0769/MycrhN_3064 of *M. rhodesiae* (S4 Figure). The other protein, MMASJCM_4343, is orthologous to UfaA1 (cyclopropane fatty acid synthase), which is present in a part of RGM and SGM species. The function of UfaA1 in mycolate biosynthesis is not clear [34]. The massiliense cluster has two unique mycolic acid synthesis-associated proteins that are not present in the abscessus or bolletii clusters.

Conclusions

The *M. abscessus* group is classified as RGM species and consists of three closely related organisms, *M. abscessus*, *M. bolletii* and *M. massiliense*. A comparative analysis based on three clusters in the *M. abscessus* group revealed that a genomic island MmGI-1 of *M. massiliense* may be involved in high growth potential with additional lipid metabolism such as putative β -oxidation pathway. Moreover, MmGI-1 is conserved in *Actinomycetales*, especially *Mycobacterium*, and horizontal gene transfer or genetic recombination events might have occurred within MmGI-1 among *M. massiliense* and MAC. Although *M. abscessus* subsp. is an environmental organism found in soil, water and other ecological niches, the difference of detail ecological niches is still unclear among subspecies-level. Our data suggests that the massiliense cluster unique regions including MmGI-1 might be linked to differences in ecological niches, such as lipid rich environment, of *M. massiliense* and *M. abscessus*. Further studies are required to understand the specific genetic features identified in this study.

Materials and Methods

Bacterial strains

We sequenced *Mycobacterium massiliense* type strain JCM 15300 (CCUG 48898), which was originally isolated from the sputum of a 50-year-old woman with an 8-year history of bronchiectasis and hemoptysis [35]. This strain was obtained from the Japan Collection of Microorganisms at the Riken BioResource Center (BRC-JCM; Saitama, Japan) on September 18, 2009.

Short-read DNA sequencing

An *M. massiliense* strain DNA library (insert size of ~600 bp) was prepared using the Nextera DNA Sample Prep Kit (Illumina-compatible) (EPICENTRE Biotechnologies, Madison, WI). DNA clusters were generated on a slide using the Cluster Generation Kit (ver. 4) on an Illumina Cluster Station (Illumina, San

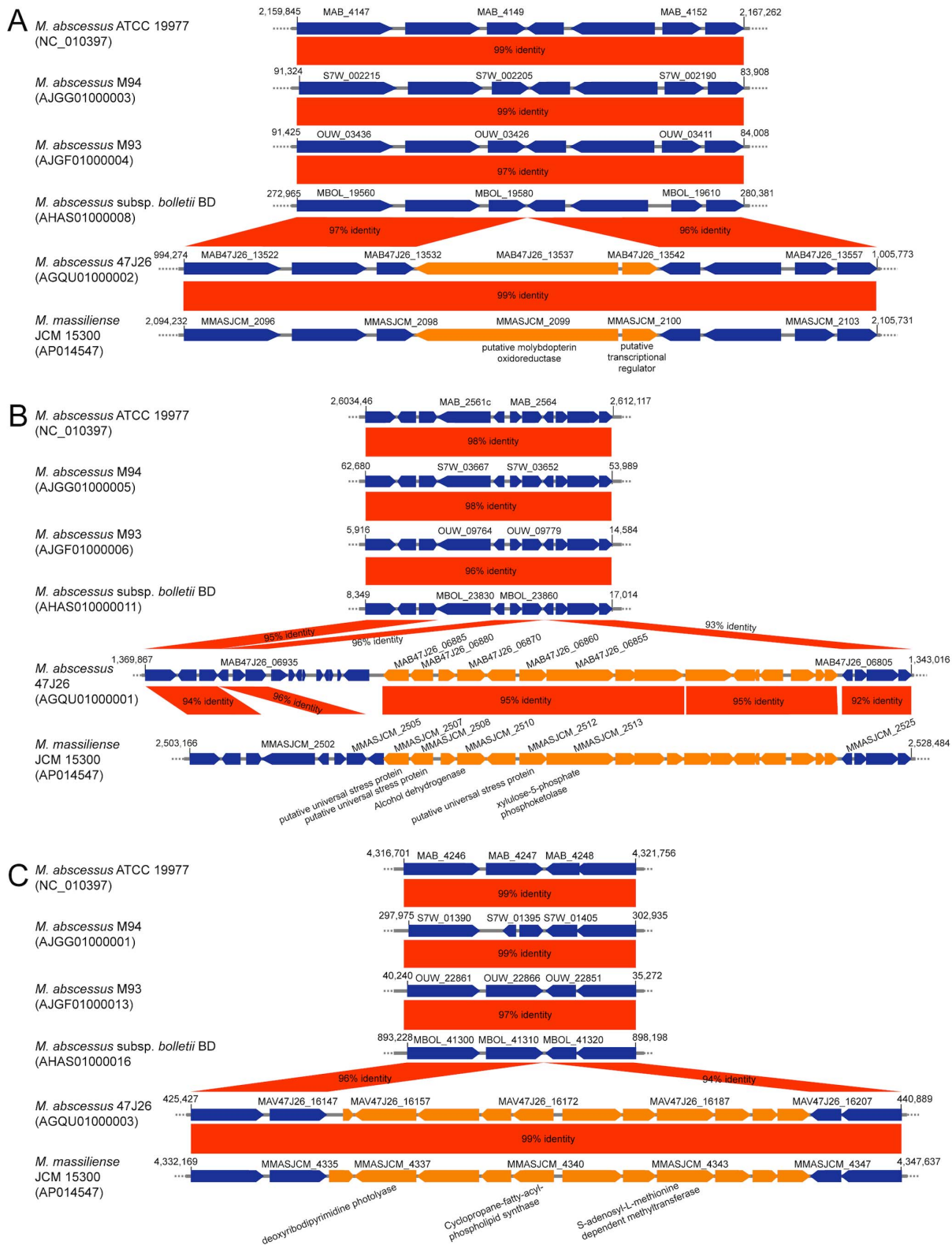


Fig. 4. Comparison of unique genes and flanking regions in the massiliense cluster. GenBank accession numbers are given in parentheses. The orange arrows indicate the unique genes in the massiliense cluster. BLASTN match scores less than 200 are not shown.

doi:10.1371/journal.pone.0114848.g004

Diego, CA), according to the manufacturer’s instructions. A paired-end sequencing run for 83 mers was performed using an Illumina Genome Analyzer IIx (GA IIx) with the TruSeq SBS Kit v5. Fluorescent images were analyzed using the Illumina RTA1.8/SCS2.8 base-calling pipeline to obtain FASTQ-formatted sequence data.

De novo assembly of short DNA reads and gap-closing

Prior to *de novo* assembly, the obtained 80-mer reads were assembled using ABySS-pe v1.2.5 [36] with the following parameters: k60, n60, c68.4, t10, e10 and q20. Predicted gaps were amplified with specific PCR primer pairs followed by Sanger DNA sequencing with the BigDye Terminator v3.1 Cycle Sequencing Kit (Applied Biosystems, Foster City, CA).

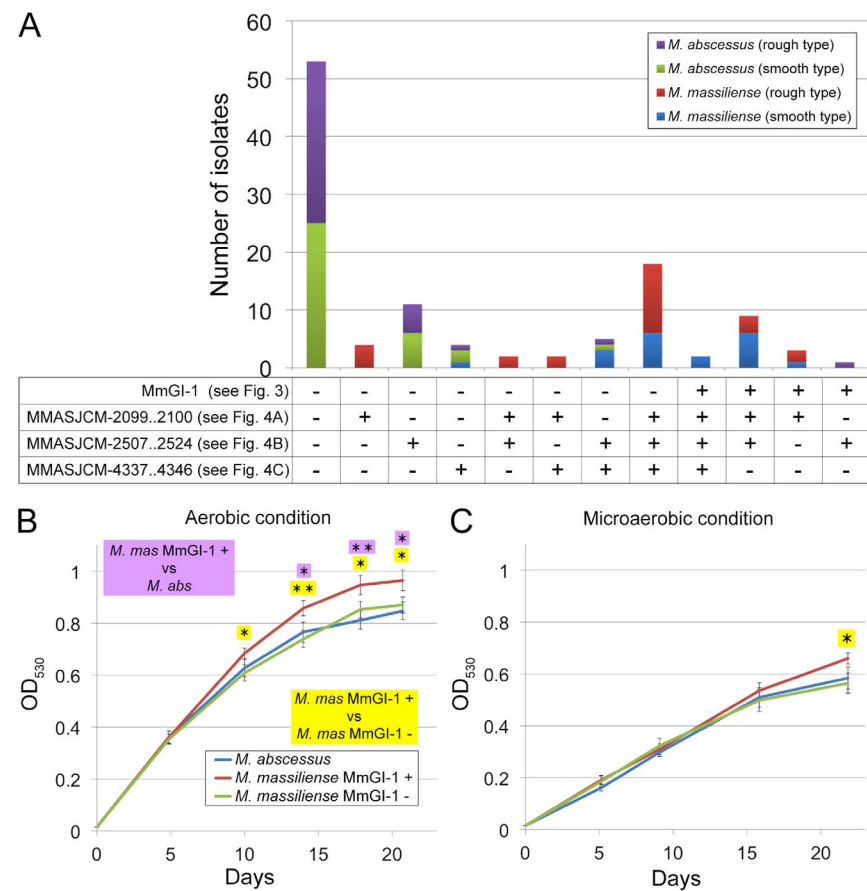


Fig. 5. Prevalence of massiliense cluster unique regions and growth curve analysis in Japanese *M. massiliense* and *M. abscessus* isolates. A bar chart showing the prevalence of MmGI-1 and three massiliense cluster unique regions in Japanese *M. massiliense* and *M. abscessus* isolates (A). The curves represent *in vitro* growth (OD at 530 nm) over a period of 21 days at 37°C in aerobic (B) and microaerobic (C) conditions. Data represent the means ± SE from 6 MmGI-1 positive *M. massiliense*, 8 MmGI-1 negative *M. massiliense* and 12 *M. abscessus* isolates. *M. mas* and *M. abs* shows *M. massiliense* and *M. abscessus*, respectively. Key: +, positive; -, negative. * $P < 0.05$; ** $P < 0.01$ (Student’s t-test).

doi:10.1371/journal.pone.0114848.g005

Validation of gap closing and sequencing errors by short-read mapping

To determine whether mis-assembled sequences and incorrect gap-closing remained after reference-assisted gap-closing, 40-mer short reads were aligned to the tentative complete chromosomal DNA sequence using Maq software (ver. 0.7.1) with the `easyrun` Perl command [37]. We then performed a read alignment to validate possible errors using the MapView graphical alignment viewer [38].

Annotation

Gene prediction was performed for the complete genomic sequence with the RAST annotation server [39], followed by InterProScan [40] search and BLASTP search using nr database for validation. Genomic information, such as nucleotide variations and circular representations, was analyzed with gview software [41].

Pairwise alignment of chromosomal sequences

Pairwise alignment was performed by BLASTN and TBLASTN homology searches [42] followed by visualization of the aligned images with the ACT [43] or EMBOSS `dottup` program [44].

BLAST atlas

A BLAST atlas was generated by a BLASTP homology search [42] using the gview program [41]. The atlas displays BLASTP comparison results. The visualized area shows that the length of similar genes covers at least 80% between *M. massiliense* JCM 15300 and other *Mycobacterium* spp.

SNP analysis

To construct simulated paired-end reads from the available genomic sequences of *M. abscessus* group strains, SimSeq software [45] was used with “`SimSeq.jar`” and “`SamToFastq.jar`” commands with the following default parameter modifications: number of pairs of reads, “`—read_number 2000000`”; mean library insert size, “`—insert_size 150`”; and paired-end reads length of 120 mer, “`—1 120 —2 120`”. These parameters indicated that 4 million hypothetical 120-mer reads were generated without mutations or indels from the genomic sequences used for SNP identification. To generate short-read mapping data of all *M. abscessus* group strains compared with the reference chromosomal sequence of *M. massiliense* JCM 15300, `bwasw` [46] and `samtools` [47] software was used with the default parameters. All SNPs were extracted by VarScan v2.3.4 [48] with the default parameters. All SNPs were concatenated to generate a pseudo sequence for phylogenetic analysis. The DNA maximum-likelihood program (RAxML v7.25) [49] was used for phylogenetic analysis with 1,000-fold bootstrapping. FigTree v. 1.2.3 software was used to display the generated tree.

Phylogenetic analysis

Nucleotide and amino acid sequences were aligned with mafft v6.86 [50] followed by phylogenetic analysis using the neighbor-joining method or maximum-likelihood method with 1,000-fold bootstrapping in clustalW2 [51] or RAxML v7.2.5 software [49]. FigTree v. 1.2.3 software was used to display the generated tree.

PCR amplification

The PCR mixture contained approximately 1 ng of template DNA, 1 × PrimeSTAR GXL Buffer (Takara Biochem. Shiga, Japan), 200 μM of each dNTP, 200 nM of each primer, and a total of 2.5 unit of PrimeSTAR GXL DNA polymerase (Takara Biochem.). The primer sequences for PCR amplification are shown in S4 Table. PCR was performed in 25 μl volumes under the following conditions: at 98°C for 20 sec followed by 30 cycles at 98°C for 15 sec, 65°C for 15 sec and 68°C for 1 min (for below 1.5 kb amplicons) or 5 min (for over 1.5 kb amplicons). Amplified PCR products were electrophoresed in 1.0% (w/v) agarose gel at 100 V and detected by staining with GelRed (Biotium Inc. Hayward, CA).

Bacterial culture

The *M. abscessus* and *M. massiliense* type strains were cultured at 37°C in Middlebrook 7H9 broth (Difco) supplemented with 10% OADC (BD) and 0.05% Tween 80 under aerobic or microaerobic (6% aerobic O₂ tension) conditions with AnaeroPack (Mitsubishi Gas Chemical Company, Inc., Tokyo, Japan). Growth was monitored by removing aliquots at the indicated time points and measuring the OD at 530 nm.

Statistical analysis

The statistical test between MmGI-1 positive *M. massiliense* and *M. abscessus* was calculated by Fisher's Exact Test. Data of bacterial culture are expressed as mean ± standard error (SE) from 7 MmGI-1 positive *M. massiliense*, 8 MmGI-1 negative *M. massiliense* and 12 *M. abscessus* isolates. Statistical analysis was performed using the student's t-test. The t-test was used to investigate whether the means of two groups are statistically different from each other. Differences were considered significant with a p-value of <0.05 and 0.01.

Nucleotide sequence accession numbers

The complete genomic sequence of *M. massiliense* JCM 15300 has been deposited into the DNA Data Bank of Japan (DDBJ; accession number: AP014547).

Supporting Information

S1 Figure. Comparative analysis between the complete genomic sequence of the *M. massiliense* JCM 15300 strain and draft genomic sequences of *M. massiliense* CCUG 48898. The upper dot plot represents synteny between JCM 15300 and CCUG 48898, and the yellow vertical bars indicate gap regions in the draft genome of CCUG 48898. The bottom table shows gaps between contigs in CCUG 48898.

[doi:10.1371/journal.pone.0114848.s001](https://doi.org/10.1371/journal.pone.0114848.s001) (TIF)

S2 Figure. Genomic comparison and BLAST atlas of 3 clusters in the *M. abscessus* group. Comparative analysis of *M. massiliense* JCM 15300 and *M. abscessus* ATCC 19977 using a BLASTN homology search visualized by the ACT program (middle) and a BLAST atlas of *M. massiliense* JCM 15300 and *M. abscessus* ATCC 19977. In the comparative analysis, the red and blue bars between chromosomal DNA sequences represent nucleotide matches in the forward and reverse directions, respectively. BLASTN match scores less than 999 are not shown. In the BLAST atlas, the coding regions of JCM 15300 or ATCC 19977 were aligned against those of other *M. abscessus* group strains using BLASTP, and the results are displayed as colored bars (as in Fig. 1A). The three yellow boxes represent prophages on each chromosome. Specific features are represented by characters: †, unique region in the massiliense cluster; •, unique region in JCM 15300; §, unique region in the abscessus cluster; ¶, MmGI-1 (also see blue bars in Fig. 1A).

[doi:10.1371/journal.pone.0114848.s002](https://doi.org/10.1371/journal.pone.0114848.s002) (TIF)

S3 Figure. Visualization for *M. abscessus* group pan-genomes and core genomes. A. Curve for pan-genomes and core genomes of *M. abscessus* group. The box plots indicate the pan- or core genome size for each genome comparison. The median values were connected to represent the relationship between genome number and gene cluster number. B. Curve for the new gene cluster number observed with every increase in the number of *M. abscessus* group genomes.

[doi:10.1371/journal.pone.0114848.s003](https://doi.org/10.1371/journal.pone.0114848.s003) (TIF)

S4 Figure. Phylogenetic tree of mycolic acid cyclopropane synthetase domain (CMAS, pfam02353) proteins in *Mycobacterium* using the maximum-likelihood method with 1,000-fold bootstrapping. The scale indicates that a branch length of 0.3 is 30 times as long as one that would show a 1% difference between the amino acid sequences at the beginning and end of the branch. The number at each branch node represents the bootstrapping value. The proteins in red indicate proteins that are conserved only in the massiliense cluster.

[doi:10.1371/journal.pone.0114848.s004](https://doi.org/10.1371/journal.pone.0114848.s004) (TIF)

S1 Table. Mutation sites in the complete genomic sequence of *M. massiliense* JCM 15300 compared with those in draft genomic sequences of *M. massiliense* CCUG 48898.

[doi:10.1371/journal.pone.0114848.s005](https://doi.org/10.1371/journal.pone.0114848.s005) (PDF)

S2 Table. The unique gene loci in *M. massiliense* JCM15300.

[doi:10.1371/journal.pone.0114848.s006](https://doi.org/10.1371/journal.pone.0114848.s006) (PDF)

S3 Table. The deleted genes of massiliense and bolletii clusters among *M. abscessus* group.

[doi:10.1371/journal.pone.0114848.s007](https://doi.org/10.1371/journal.pone.0114848.s007) (PDF)

S4 Table. Oligonucleotide primer sequences used in PCR assays and the judging method for presence of MmGI-1 and other *M. massiliense* unique regions.

[doi:10.1371/journal.pone.0114848.s008](https://doi.org/10.1371/journal.pone.0114848.s008) (PDF)

S5 Table. Isolates analyzed in the present study and results of conventional PCR based detection against MmGI-1 and other *M. massiliense* unique regions.

[doi:10.1371/journal.pone.0114848.s009](https://doi.org/10.1371/journal.pone.0114848.s009) (PDF)

Author Contributions

Conceived and designed the experiments: TS M. Kai YH M. Kuroda. Performed the experiments: TS M. Kai KN NN YK SM YH M. Kuroda. Analyzed the data: TS M. Kai M. Kuroda. Contributed reagents/materials/analysis tools: TS M. Kai MM YH M. Kuroda. Wrote the paper: TS M. Kuroda. Performed genomic sequencing: TS M. Kai M. Kuroda.

References

1. Griffith DE, Aksamit T, Brown-Elliott BA, Catanzaro A, Daley C, et al. (2007) An official ATS/IDSA statement: diagnosis, treatment, and prevention of nontuberculous mycobacterial diseases. *American journal of respiratory and critical care medicine* 175: 367–416.
2. Brown-Elliott BA, Nash KA, Wallace RJ Jr (2012) Antimicrobial susceptibility testing, drug resistance mechanisms, and therapy of infections with nontuberculous mycobacteria. *Clinical microbiology reviews* 25: 545–582.
3. Olivier KN, Weber DJ, Wallace RJ Jr, Faiz AR, Lee JH, et al. (2003) Nontuberculous mycobacteria. I: multicenter prevalence study in cystic fibrosis. *American journal of respiratory and critical care medicine* 167: 828–834.
4. Bryant JM, Grogono DM, Greaves D, Foweraker J, Roddick I, et al. (2013) Whole-genome sequencing to identify transmission of *Mycobacterium abscessus* between patients with cystic fibrosis: a retrospective cohort study. *Lancet* 381: 1551–1560.
5. Iseman MD, Marras TK (2008) The importance of nontuberculous mycobacterial lung disease. *American journal of respiratory and critical care medicine* 178: 999–1000.
6. Chan ED, Bai X, Kartalija M, Orme IM, Ordway DJ (2010) Host immune response to rapidly growing mycobacteria, an emerging cause of chronic lung disease. *American journal of respiratory cell and molecular biology* 43: 387–393.
7. Falkinham JO 3rd (1996) Epidemiology of infection by nontuberculous mycobacteria. *Clinical microbiology reviews* 9: 177–215.
8. Primm TP, Lucero CA, Falkinham JO 3rd (2004) Health impacts of environmental mycobacteria. *Clinical microbiology reviews* 17: 98–106.
9. Bastian S, Veziris N, Roux AL, Brossier F, Gaillard JL, et al. (2011) Assessment of clarithromycin susceptibility in strains belonging to the *Mycobacterium abscessus* group by *erm*(41) and *rrl* sequencing. *Antimicrobial agents and chemotherapy* 55: 775–781.

10. **Macheras E, Roux AL, Bastian S, Leao SC, Palaci M, et al.** (2011) Multilocus sequence analysis and *rpoB* sequencing of *Mycobacterium abscessus* (*sensu lato*) strains. *Journal of clinical microbiology* 49: 491–499.
11. **Nakanaga K, Sekizuka T, Fukano H, Sakakibara Y, Takeuchi F, et al.** (2014) Discrimination of *Mycobacterium abscessus* subsp. *massiliense* from *Mycobacterium abscessus* subsp. *abscessus* in Clinical Isolates by Multiplex PCR. *Journal of clinical microbiology* 52: 251–259.
12. **Furuya EY, Paez A, Srinivasan A, Cooksey R, Augenbraun M, et al.** (2008) Outbreak of *Mycobacterium abscessus* wound infections among "lipotourists" from the United States who underwent abdominoplasty in the Dominican Republic. *Clinical infectious diseases: an official publication of the Infectious Diseases Society of America* 46: 1181–1188.
13. **Medjahed H, Gaillard JL, Reytrat JM** (2010) *Mycobacterium abscessus*: a new player in the mycobacterial field. *Trends in microbiology* 18: 117–123.
14. **Villanueva A, Calderon RV, Vargas BA, Ruiz F, Agüero S, et al.** (1997) Report on an outbreak of postinjection abscesses due to *Mycobacterium abscessus*, including management with surgery and clarithromycin therapy and comparison of strains by random amplified polymorphic DNA polymerase chain reaction. *Clinical infectious diseases: an official publication of the Infectious Diseases Society of America* 24: 1147–1153.
15. **Otsuki T, Izaki S, Nakanaga K, Hoshino Y, Ishii N, et al.** (2012) Cutaneous *Mycobacterium massiliense* infection: a sporadic case in Japan. *The Journal of dermatology* 39: 569–572.
16. **Nakanaga K, Hoshino Y, Era Y, Matsumoto K, Kanazawa Y, et al.** (2011) Multiple cases of cutaneous *Mycobacterium massiliense* infection in a "hot spa" in Japan. *Journal of clinical microbiology* 49: 613–617.
17. **Cho YJ, Yi H, Chun J, Cho SN, Daley CL, et al.** (2013) The Genome Sequence of 'Mycobacterium massiliense' Strain CIP 108297 Suggests the Independent Taxonomic Status of the *Mycobacterium abscessus* Complex at the Subspecies Level. *PLoS one* 8: e81560.
18. **Ripoll F, Pasek S, Schenowitz C, Dossat C, Barbe V, et al.** (2009) Non mycobacterial virulence genes in the genome of the emerging pathogen *Mycobacterium abscessus*. *PLoS one* 4: e5660.
19. **Choo SW, Wee WY, Ngeow YF, Mitchell W, Tan JL, et al.** (2014) Genomic reconnaissance of clinical isolates of emerging human pathogen *Mycobacterium abscessus* reveals high evolutionary potential. *Sci Rep* 4: 4061.
20. **Pawlik A, Garnier G, Orgeur M, Tong P, Lohan A, et al.** (2013) Identification and characterization of the genetic changes responsible for the characteristic smooth-to-rough morphotype alterations of clinically persistent *Mycobacterium abscessus*. *Mol Microbiol* 90: 612–629.
21. **Joseph J, Rajendran V, Hassan S, Kumar V** (2011) *Mycobacteriophage* genome database. *Bioinformatics* 6: 393–394.
22. **Casali N, Riley LW** (2007) A phylogenomic analysis of the Actinomycetales *mce* operons. *BMC genomics* 8: 60.
23. **Arruda S, Bomfim G, Knights R, Huima-Byron T, Riley LW** (1993) Cloning of an *M. tuberculosis* DNA fragment associated with entry and survival inside cells. *Science* 261: 1454–1457.
24. **Pandey AK, Sassetti CM** (2008) Mycobacterial persistence requires the utilization of host cholesterol. *Proceedings of the National Academy of Sciences of the United States of America* 105: 4376–4380.
25. **Klepp LI, Forrellad MA, Osella AV, Blanco FC, Stella EJ, et al.** (2012) Impact of the deletion of the six *mce* operons in *Mycobacterium smegmatis*. *Microbes and infection/Institut Pasteur* 14: 590–599.
26. **Kim SH, Harzman C, Davis JK, Hutcheson R, Broderick JB, et al.** (2012) Genome sequence of *Desulfotobacterium hafniense* DCB-2, a Gram-positive anaerobe capable of dehalogenation and metal reduction. *BMC microbiology* 12: 21.
27. **Suzuki R, Katayama T, Kim BJ, Wakagi T, Shoun H, et al.** (2010) Crystal structures of phosphoketolase: thiamine diphosphate-dependent dehydration mechanism. *The Journal of biological chemistry* 285: 34279–34287.
28. **Boes N, Schreiber K, Hartig E, Jaensch L, Schobert M** (2006) The *Pseudomonas aeruginosa* universal stress protein PA4352 is essential for surviving anaerobic energy stress. *Journal of bacteriology* 188: 6529–6538.

29. **Klotz T, Vorreuther R, Heidenreich A, Zumbe J, Engelmann U** (1996) Testicular tissue oxygen pressure. *The Journal of urology* 155: 1488–1491.
30. **Shahidi M, Wanek J, Blair NP, Little DM, Wu T** (2010) Retinal tissue oxygen tension imaging in the rat. *Investigative ophthalmology & visual science* 51: 4766–4770.
31. **Wang W, Vadgama P** (2004) O₂ microsensors for minimally invasive tissue monitoring. *Journal of the Royal Society, Interface/the Royal Society* 1: 109–117.
32. **Ponce LL, Pillai S, Cruz J, Li X, Julia H, et al.** (2012) Position of probe determines prognostic information of brain tissue PO₂ in severe traumatic brain injury. *Neurosurgery* 70: 1492–1502; discussion 1502–1493.
33. **Barkan D, Rao V, Sukenick GD, Glickman MS** (2010) Redundant function of *cmaA2* and *mmaA2* in *Mycobacterium tuberculosis* cis cyclopropanation of oxygenated mycolates. *Journal of bacteriology* 192: 3661–3668.
34. **Banerjee R, Vats P, Dahale S, Kasibhatla SM, Joshi R** (2011) Comparative genomics of cell envelope components in mycobacteria. *PLoS one* 6: e19280.
35. **Adekambi T, Reynaud-Gaubert M, Greub G, Gevaudan MJ, La Scola B, et al.** (2004) Amoebal coculture of "*Mycobacterium massiliense*" sp. nov. from the sputum of a patient with hemoptoic pneumonia. *Journal of clinical microbiology* 42: 5493–5501.
36. **Simpson JT, Wong K, Jackman SD, Schein JE, Jones SJ, et al.** (2009) ABySS: a parallel assembler for short read sequence data. *Genome research* 19: 1117–1123.
37. **Li H, Ruan J, Durbin R** (2008) Mapping short DNA sequencing reads and calling variants using mapping quality scores. *Genome research* 18: 1851–1858.
38. **Bao H, Guo H, Wang J, Zhou R, Lu X, et al.** (2009) MapView: visualization of short reads alignment on a desktop computer. *Bioinformatics* 25: 1554–1555.
39. **Aziz RK, Bartels D, Best AA, DeJongh M, Disz T, et al.** (2008) The RAST Server: rapid annotations using subsystems technology. *BMC genomics* 9: 75.
40. **Jones P, Binns D, Chang HY, Fraser M, Li W, et al.** (2014) InterProScan 5: genome-scale protein function classification. *Bioinformatics* 30: 1236–1240.
41. **Petkau A, Stuart-Edwards M, Stothard P, Van Domselaar G** (2010) Interactive microbial genome visualization with GView. *Bioinformatics* 26: 3125–3126.
42. **Altschul SF, Gish W, Miller W, Myers EW, Lipman DJ** (1990) Basic local alignment search tool. *Journal of molecular biology* 215: 403–410.
43. **Carver TJ, Rutherford KM, Berriman M, Rajandream MA, Barrell BG, et al.** (2005) ACT: the Artemis Comparison Tool. *Bioinformatics* 21: 3422–3423.
44. **Rice P, Longden I, Bleasby A** (2000) EMBL-EBSS: the European Molecular Biology Open Software Suite. *Trends in genetics: TIG* 16: 276–277.
45. **Earl D, Bradnam K, St John J, Darling A, Lin D, et al.** (2011) Assemblathon 1: a competitive assessment of de novo short read assembly methods. *Genome research* 21: 2224–2241.
46. **Li H, Durbin R** (2010) Fast and accurate long-read alignment with Burrows-Wheeler transform. *Bioinformatics* 26: 589–595.
47. **Li H** (2011) A statistical framework for SNP calling, mutation discovery, association mapping and population genetical parameter estimation from sequencing data. *Bioinformatics* 27: 2987–2993.
48. **Koboldt DC, Chen K, Wylie T, Larson DE, McLellan MD, et al.** (2009) VarScan: variant detection in massively parallel sequencing of individual and pooled samples. *Bioinformatics* 25: 2283–2285.
49. **Stamatakis A** (2006) RAxML-VI-HPC: maximum likelihood-based phylogenetic analyses with thousands of taxa and mixed models. *Bioinformatics* 22: 2688–2690.
50. **Katoh K, Toh H** (2010) Parallelization of the MAFFT multiple sequence alignment program. *Bioinformatics* 26: 1899–1900.
51. **Larkin MA, Blackshields G, Brown NP, Chenna R, McGettigan PA, et al.** (2007) Clustal W and Clustal X version 2.0. *Bioinformatics* 23: 2947–2948.